



## STRUCTURAL MITIGATION OF BUILDINGS DAMAGED BY THE 2011 TOHOKU TSUNAMI USING THE ASCE 7 TSUNAMI DESIGN PROVISIONS

L.P. Carden<sup>(1)</sup>, G.Y.K. Chock<sup>(2)</sup>

<sup>(1)</sup> Principal, Martin & Chock, Inc. [lcarden@martinchock.com](mailto:lcarden@martinchock.com)

<sup>(2)</sup> President, Martin & Chock, Inc. [gchock@martinchock.com](mailto:gchock@martinchock.com)

### **Abstract**

A number of building tsunami failures were analyzed by an ASCE tsunami reconnaissance team after the devastating Great East Japan Earthquake and Tohoku Tsunami of March 11, 2011. In previous studies by the authors, structural failures of buildings were analytically replicated from their structural response, as calculated for field-estimated maximum flow depths and velocities. The structures were selected for a range of effects, including buoyancy, lateral hydrostatic, hydrodynamic and debris damming loading conditions. Overall, the analyses demonstrated that the ASCE 7 tsunami design provisions are sufficiently reliable engineering design tools for structural load characterization and analysis of suitably defined tsunami flow conditions.

In this paper, possible modifications to the examples of damaged structures are developed based on the ASCE 7 tsunami design provisions, together with a discussion of the mitigation options to upgrade various types of structures for tsunami resistance. These example buildings are retrospectively used to demonstrate design strategies to achieve tsunami resiliency of buildings based on tsunami flow characteristics observed at different sites during the Tohoku Tsunami, which represent relatively extreme tsunami design criteria. Resistance to hydrostatic buoyancy forces may be achieved by several approaches, selected depending on performance objective. The methods include installation of deep foundations with sufficient tensile capacity to resist a buoyant condition of a structure and/or to preclude pressurization of the underlying soil. Alternatively, the structure may be designed to relieve hydrostatic uplift pressures through breakaway slabs or sacrificial exterior wall or cladding elements, allowing internal flooding of the building. Components of a structural steel frame building can be feasibly designed for additional lateral resistance to resist the hydrostatic and hydrodynamic lateral loads, including accumulated debris damming and impact effects when the inundation height is at or around the building height for the low rise building studied. There are similar mitigation techniques for concrete frame structures. Concrete structural walls can be designed to resist in-plane tsunami forces and out-of-plane forces, including bore and debris impacts, with an increase in the out-of-plane strength generally being required. The analysis demonstrates that when buildings are significantly overtopped it is difficult to design wall elements for tsunami loads. When tsunami inundation depth is not more than the height of concrete or steel framed structure, it can be more feasibly designed for tsunami forces. Special debris impact loads are not considered.

*Keywords: ASCE7, Tohoku, Tsunami, Design, Disaster Resilience*



## 1. Introduction

In the aftermath of the Great East Japan Earthquake of March 11, 2011 (also known as the Tohoku-Oki Earthquake), and devastating Tohoku Tsunami, access to real-time and recorded observations allowed unprecedented analysis of the tsunami and its effects. Structural damage from the tsunami was widespread throughout cities and towns along the entire Tohoku (northeast) region of Honshu Island. Damage was observed and documented for all manner of structures, including residential and commercial buildings [1, 2, 3, 4, 5], roads and bridges [6, 7] and other infrastructure.

Analysis following the tsunami synthesized visual observations, to document structural damage and maximum inundation levels; video analysis, to observe flow rates, inundation time histories, and debris flow [3, 8, 9]; satellite imaging [10], before and after the event to document inundation limits and damage patterns, and; LIDAR imaging [11], which allows three-dimensional snapshots of damaged areas, measurement of structural deformations and capture of data for future analysis. This analysis enabled the impacts on structures to be better understood with regards to the associated tsunami inundation height, flow velocity, and other characteristics relating to structural loads.

For those who have witnessed and studied the devastating impacts of the Tohoku Tsunami along with similar impacts from the 2010 Chile Tsunami [12, 13], 2007 Samoa Tsunami and 2004 Indian Ocean Tsunami, the need to increase preparedness and improve resilience for future events is apparent. Preparedness includes disaster response education, warning systems, and evacuation planning, as well as community planning and structural design of critical infrastructure and select buildings, that finds an appropriate balance between life safety, initial economic cost, and post-disaster recovery with economic resilience.

Recognizing the possible impacts of tsunamis in the United States from events such as a rupture at the Cascadia subduction zone [14] or other locations, a Tsunami Loads and Effects chapter has been incorporated in the latest update of the ASCE 7 Standard, Minimum Design Loads and Associated Criteria for Buildings and Other Structures [15]. This newly developed standard is henceforth referred to simply as ASCE 7. The purpose of this chapter is to provide a structural design standard for select buildings and infrastructure appropriate for a region's probabilistic tsunami hazard, while not disproportionately increasing the cost of a building compared to the benefits of mitigating the tsunami risk.

The design of structures for tsunamis is still an emerging practice, and some analytical effort and experience is needed to determine what structures can and cannot be reasonably designed for tsunamis. It is evident from post-tsunami observations that low rise, light framed structures, typical of single or small multi-family residences, cannot be readily designed for significant tsunami inundation, while other structural steel and concrete structures can be designed to survive for life safety or higher performance levels. The tsunami design requirements of ASCE 7 apply to Risk Category III and IV buildings and structures (that is select high occupancy buildings and critical and essential facilities) where located within a Tsunami Design Zone (TDZ) in the coastal areas of Alaska, Washington, Oregon, California, and Hawaii. Risk Category III and IV represent a relatively small proportion of the buildings in the TDZ. It is much preferred that these types of buildings be located outside or towards the landward edge of the TDZ if at all practical. Nevertheless, it is probable that a significant number of important structures may be required to exist within a TDZ, such as where the function of the facility requires it to be near the coastline, where the economy of the community is related to its access to the ocean, where either the available land area is limited or the hazard area is broad due to topography, or a specifically designed tsunami evacuation shelter.

It is the opinion of the authors that the tsunami design provisions should also apply to certain mid-rise and high-rise Risk Category II buildings, i.e. those with residential, commercial, hotel or other common building occupancies. This opinion is based on the expectation based on analysis that taller buildings would provide safety above the inundation level and that it is generally not expected to take much strengthening to design the lower levels of a multi-story building for a life safety tsunami design performance objective [16]. There are many communities in the Tsunami Design Zone where complete evacuation cannot be assured prior to tsunami arrival; the consequences of being caught on the ground during a tsunami are near certainly fatal. Therefore, in



the adoption of the tsunami design standard of ASCE 7, local jurisdictions may choose to expand its applicability accordingly in their local building code to create “fortresses of safety” as a part of their future multi-story building inventory.

A previous study analyzed a number of structures located in various inundated regions of the coastline in the Miyagi and Iwate Prefectures of Japan for the calculated tsunami loads based on estimates of flow depth and velocities during the 2011 Tohoku Tsunami [16]. The structures were selected for a range of buoyancy, lateral hydrostatic, hydrodynamic, and accumulated debris loading conditions. A further study investigated how well the damage would have been captured compared to the design standards of ASCE 7 Tsunami design provisions, knowing just the maximum runup elevation [5]. The methods of ASCE 7 were used to calculate site specific inundation depth and velocities, along with the associated loading on the structures. It found that the standard provided a robust and generally conservative design methodology for calculating tsunami loading on structures. This study takes the analysis a step further to study ways the buildings could have been designed for effects of the tsunami. The purpose of the program of study is to add to the understanding of what modifications to structures are needed for improving the performance of buildings during a tsunami using the experience from tsunami reconnaissance that cannot be acquired analytically or in laboratories.

## 2. ASCE 7 Tsunami Loads and Effects Design Provisions

Typical definitions used in defining tsunami inundation characteristics are provided in Fig. 1. These definitions are reproduced from ASCE 7 and used throughout.

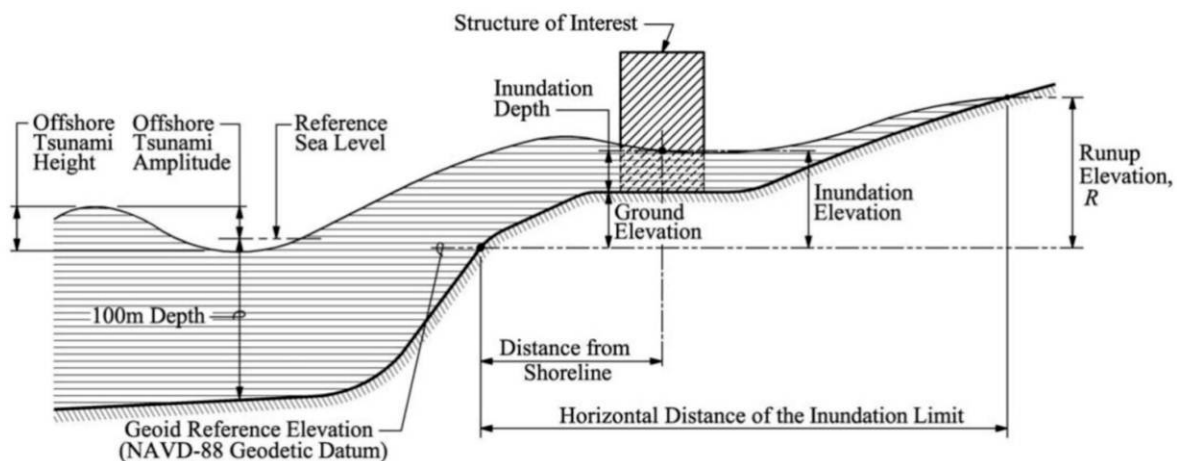


Fig. 1 - Illustration of Key Definitions along a Flow Transect in a Tsunami Design Zone [15]

There are two procedures for determining the tsunami inundation or flow depth and velocities at a site:

- (1) The Energy Grade Line Analysis, which takes the runup elevation and inundation limit indicated on the Tsunami Design Zone map to conservatively stipulate the inundation depth and hydraulic characteristics at a given site, applicable to the design of all buildings, and
- (2) A two-dimensional Site-Specific Inundation Analysis, if as preferred for greater accuracy by a designer.

Three cases of tsunami structural loading must be considered, defined by inundation depths and their associated velocities. The maximum inundation depth and velocity do not occur simultaneously. The velocity is generally largest as the water inundates and recedes but approaches zero at the point of maximum inundation when the tsunami flow changes direction. The three cases consider:

- (1) Differential hydrostatic, buoyancy and hydrodynamic forces between the exterior and interior of an enclosed building up to a height of one story or to the top of the first story windows, but not greater than the maximum inundation depth of the tsunami;



- (2) Two-thirds of the maximum inundation depth along with maximum velocity;
- (3) Near maximum inundation depth with one-third of the maximum velocity.

These cases shall consider multiple cycles of flow that include scour effects, debris accumulation, and variations in the primary direction of loading. Tsunami loads should also be combined with the inherent gravity loads in combinations similar to those for earthquake loads as defined in ASCE 7.

The main lateral force-resisting system should be designed for the overall pressure loading at an ultimate load level for the load cases described above. In high seismic zones where a structure is detailed for ductility and structural integrity of the load path, the overall system capacity will be considered acceptable without additional analysis provided the total tsunami lateral force acting on the structure is less than 75% of the horizontal seismic loads including the system seismic overstrength factor,  $\Omega_o$ .

The components of the building must have the necessary design strength for tsunami pressures of ASCE 7 calculated for the different load cases. If the acceptance criteria for an individual component are exceeded, as an alternative to an upgraded design, it is also permitted to apply progressive collapse procedures to design the structure with alternative load paths to accommodate localized failures of gravity-load-carrying members.

### **3. Observed Performance of Structures During the Tohoku Tsunami and Mitigation of Damage Using the ASCE 7 Standard**

#### **3.1 Determination of Tsunami Flow Depth and Velocity at Various Sites Using Energy Grade Line Analyses**

The ASCE 7 standard provides TDZs and the inundation limit for the probabilistic 2500-year Maximum Considered Tsunami for all U.S. Pacific coastlines. Similar maps have been or can be developed for other coastlines elsewhere to enable the application of the ASCE 7 design methodology. Knowing the design inundation limit and runup elevation, the Energy Grade Line method can be used to determine the specific design inundation depth and flow velocity to be used for design at a given site.

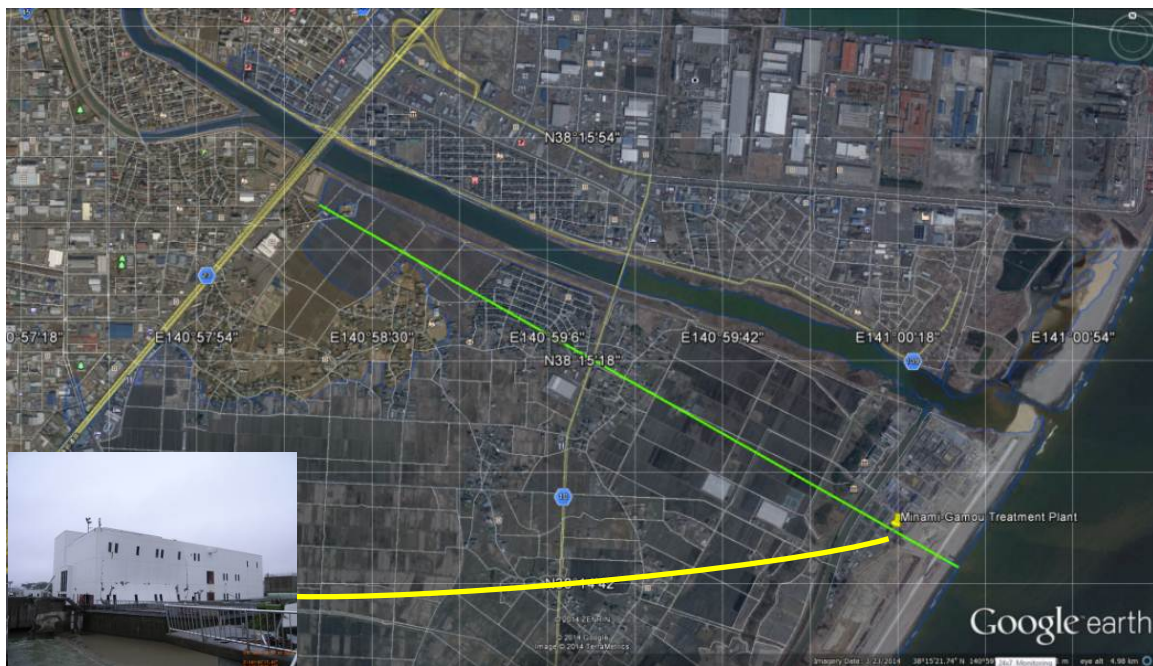
The buildings considered as case studies are located on or close to selected transects oriented perpendicular to different parts of the Tohoku coastline, in three different areas. The three areas and transects used for the ASCE 7 Energy Grade Line (EGL) analysis are shown in Fig. 2, along with the tsunami inundation zone determined from a field survey by a number of Japanese researchers [1]. The transects are located in: (a) the coastal valley township of Onagawa, and; (b) the Sendai plain, crossing the location of the Minami-Gamou Wastewater treatment plant near the coast.

The Energy Grade Line determines the variation of inundation depth and associated flow velocity across the inland profile, accounting for the effects of topographic elevation and hydraulic friction of the terrain. Velocity is assumed to be a function of inundation depth, calibrated to the Froude number that is prescribed to decay gradually based on distance from the shoreline along the transect, using the procedures described in ASCE 7 [15]. Typically, the Froude number coefficient,  $\alpha$ , is set equal to 1.0 (resulting in a Froude number of 1.0 at the shoreline where  $x = 0$ ) for areas where tsunami bore conditions do not exist. The Froude number coefficient is set at 1.3 for bore conditions.

The results of the EGL analyses, for specific sites of interest are provided in Table 1. The analysis assumes a Manning roughness of 0.040 for Onagawa and Rikuzentakata, and 0.030 for the Sendai plain. The Froude number coefficient was set at 1.0 for Onagawa and Rikuzentakata, and 1.3 for the Sendai plain based on the offshore bathymetry and survivor video evidence of tsunami bores at the Sendai side. The EGL flow characteristics are found to be generally conservative, as intended for design, when compared to the inundation depths and flow speeds determined by post-tsunami survey and calculated from video or other field evidence [16]. The design velocity is expected to be inherently around 1.5 times greater than the general flow velocity to account for localized flow velocity amplification. This approximately corresponds to the difference between calculated and observed estimated velocities. The estimate is a little more conservative for Sendai attributed to a



2(a) Onagawa



2(b) Sendai

Fig. 2. Inundation zones, EGL transects, and coastal structures of interest at a) Onagawa, b) Sendai



Table 1 - Summary of Flow Depths and Velocities at Sites from Energy Grade Lines

Site	Distance from shoreline (m)	Calculated EGL		Estimated from Survey <sup>1</sup>	
		Flow Depth (m)	Flow Velocity (m/s)	Flow Depth (m)	Flow Velocity (m/s)
<b>Onagawa</b>					
Site 1 – Overturned Concrete Bldg.	150	16.2	11.8	19	7.4-8.2
Site 2 – Steel Residential Bldg.	120	16.2	12.0		
Site 3 – Concrete Warehouse	210	16.1	11.5		
<b>Sendai</b>					
Minami-Gamou Wastewater Treatment Bldg.	330	8.2	11.1	6.0	6.5 (bore)
Notes: 1. Derived from field observations, video and other analysis [16]					

coastal berm modification to the EGL analysis required, described in the previous study [6], and also the bore condition, which is applied with a separate loading equation, discussed later. The structures at the sites represent a range of different structural types and loading conditions, as discussed in the sections to follow.

### 3.2 Tsunami Forces on Buildings

The following provides a summary of the calculated forces on buildings per ASCE 7 used for analysis throughout this study. For full discussion and the derivation of these equations refer to ASCE 7 and its commentary.

First forces that impact the building as a whole are considered. The tsunami hydrostatic uplift force is given by Eq. (1):

$$F_v = \gamma_s V_w \quad (1)$$

where  $V_w$  = volume of water displaced and  $\gamma_s$  = unit weight of water with suspended solids and smaller debris.

The hydrodynamic lateral force method, calculates the total lateral force with explicit consideration of the degree of closure of the projected wall area, as given in Eq. (2):

$$F_{dx} = \frac{1}{2} \rho_s I_{tsu} C_d C_{cx} B (hu^2) \quad (2)$$

where  $\rho_s = k_s \rho_{sw}$  (typically  $1.1(1025) = 1128 \text{ kg/m}^3$  - minimum fluid mass density for hydrodynamic loads),  $C_d$  = drag coefficient (based on the geometry of the building),  $C_{cx}$  = closure coefficient,  $B$  = building width, and  $hu^2$  = momentum flux for different combinations of flow depth and velocity.

Lateral hydrostatic forces will generally not have an impact on a structure as a whole as hydrostatic forces on one side of the building will generally be balanced by those on the other side of the building. However, lateral hydrostatic forces may have an impact on individual components such as walls and columns where the water level on one side is higher than that on the other. The lateral hydrostatic force is given by Eq. (3):

$$F_h = \frac{1}{2} \gamma_s b h_{max}^2 \quad (3)$$

The hydrodynamic drag force on building components for a non-bore condition is similar to that for the force on the main lateral-force-resisting system of the building, with adjustments to the drag coefficient to account for the



size and shape of a component acting over its width. The hydrodynamic component drag force on vertical components is given by Eq. (4):

$$F_w = \frac{1}{2} \rho_s I_{tsu} C_d b (h_s u^2) \quad (4)$$

Another possible load scenario exists for some buildings resulting from flow stagnation forces. Flow stagnation occurs in special circumstances when a hydrodynamic force acts on a part of a structure that traps a body of water that becomes pressurized, transferring these pressures to other components not directly acted on by the flow. This generally requires enclosed areas surrounded by rigid walls and slabs that are completely filled with water. This Bernoulli stagnation pressure is given by Eq. (5):

$$P_p = \frac{1}{2} \rho_s I_{tsu} u^2 \quad (5)$$

In some locations, where certain bathymetric conditions exist, the tsunami flow may reach land as a bore. This type of flow tends to carry greater energy and result in instantaneously applied hydrodynamic impact forces. The ASCE 7 provisions require the consideration of tsunami bores where any of the following five conditions exist:

1. The prevailing nearshore bathymetry slope is 1/100 or milder,
2. Shallow fringing reefs of other similar discontinuities in nearshore bathymetric slope occur,
3. Where historically documented,
4. As described in the recognized literature, or
5. As determined from site specific analysis.

Where a bore condition is deemed to exist some additional design requirements are necessary. One requirement is that the hydrodynamic drag force on wide components ( $B > 3h_e$ ) is increased by 50%, with flow depth and height based on Load Case 2, hence the force is given by Eq. (6):

$$F_w = \frac{3}{4} \rho_s I_{tsu} C_d b (h_s u^2) \quad (6)$$

### 3.3 Buildings Subject to Hydrostatic Buoyancy Forces

The reinforced concrete building shown in Fig. 3 was lifted off its pile foundation by hydrostatic buoyancy. The bearing pile connections to the pile caps were observed to have little tensile capacity as the reinforcing only extended a short way into the piles, insufficient to develop the bars. The building floated and was deposited about 15 m inland from its original location. As it was dragged, the unbalanced forces between the center of the applied tsunami pressure, and the resistance to that pressure at the ground level, caused an overturning moment. Due to the buoyancy force counteracting the gravity loads there was little resistance to the overturning moment, which caused the subsequent toppling of the building when it encountered an obstruction.

The refrigerated room portion of the ground floor was effectively sealed off without windows, allowing a differential hydrostatic pressure between the inside and outside of the building. The loading was consequently governed by ASCE 7 Load Case 1, which considers the hydrostatic force resulting from the lesser of one story, the height to the top of the windows, or the maximum inundation depth for differential inundation between the inside and outside of the building.

The net uplift force (Eq. (1)) comparing the weight of the building, with applicable load combination scale factors, was estimated at 2520kN (28% of the building weight). This was at a flow depth of 5.13m, the height of the first floor. There was also an overturning moment due to the hydrodynamic force in the direction of flow equal to 25380kNm, estimated based on the hydrodynamic force of Eq. (2) with same flow depth (5.13m) , which is equal to 32% of the maximum flow depth. At the point in the loading time history, per ASCE7 the corresponding design velocity is 80% of the maximum velocity ( $0.8 * 11.8 = 9.4\text{m/s}$ ). The building is estimated





times the capacity of the structure. As this structure survived, it was likely subject to less blockage than assumed in the analysis, but most of the similar types of structures, subject to similar loading conditions, were destroyed (and photographs showed that a portion of a collapsed steel building frame lodged itself against this building during the outflow). Considerable strengthening would be required to design this structure for this overtopping level of tsunami inundation, hence it is not likely to be cost effective. There is also little benefit since the fully inundated structure is of no use for life safety and, even if the structure was still standing after the tsunami, the restoration of the building is likely to be uneconomical.

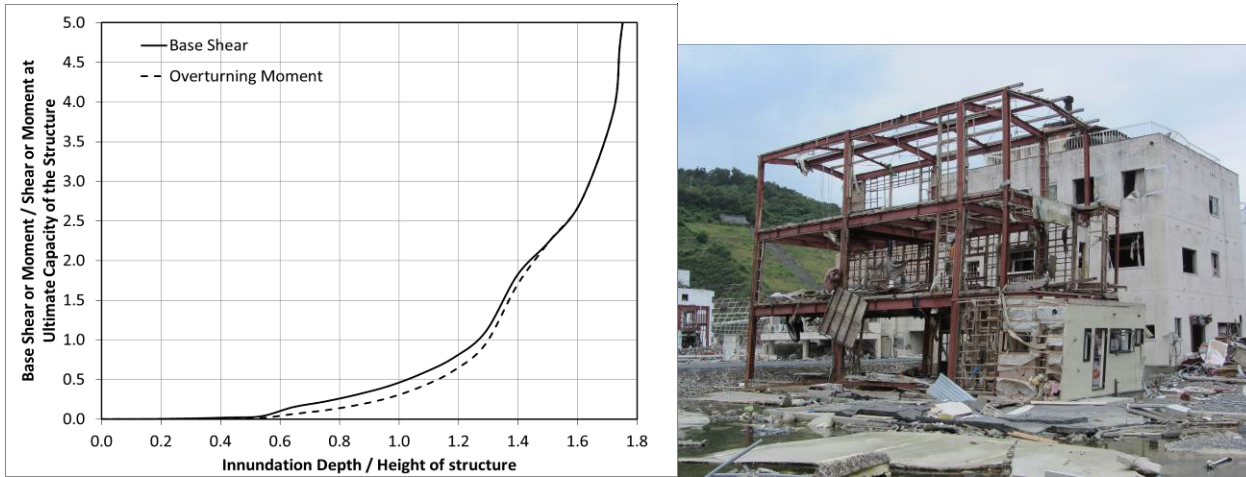


Fig. 4 - Onagawa three-story steel frame deformation during drawdown phase and plot of ratio of applied actions to capacity for different tsunami inundation depths

For lower levels of tsunami inundation depth, however, the design of this type of structure for tsunami loading becomes more feasible. Fig. 4 shows a plot of demand to capacity ratio with respect to height of the tsunami relative to the building height specific for this structure and its calculated capacity in the longitudinal direction (oriented perpendicular to the shoreline). It is based on the structure being located at different locations along the transect between the shoreline and maximum runup line, where there are different maximum inundation depths and flow velocities (based on the energy grade line). The figure shows that it is not until the tsunami inundation is over 1.3 times the height of the structure that the ultimate capacity of the structure is reached. (At larger inundation depths the forces increase almost exponentially due to be square relationship with maximum flow velocity, which also increases with maximum inundation depth.) Therefore, it is feasible to design a structure with these properties for a tsunami up to the roof of the structure, for rooftop protection of occupants. As Japan is highly seismic, the buildings have a high inherent lateral strength due to their seismic design.

### 3.5 Lateral Hydrostatic, Hydrodynamic, and Flow Stagnation Forces on Building Components

The concrete warehouse shown in Fig. 5, located in Onagawa, was used to demonstrate hydrodynamic drag and stagnation forces on components of a building, consisting of solid concrete walls. This building was particularly interesting because it had two identical panels (4.0m x 5.9m) that had failed and two slightly smaller panels (3.3m x 4.0m) that did not fail, normal to the direction of flow. It also had two of the larger sized panels, oriented parallel to the direction of flow. Thus, it served as a type of analytical instrumentation of the tsunami hydraulic forces where the inundation depth itself was determined from video documentation.

From the EGL analysis the maximum inundation depth for design at this site was estimated at 16.1 m and maximum velocity was 11.5 m/s. The depth is much greater than the height of the wall panels at 4.0m and 5.9m respectively. From previous analysis [16, 5], hydrodynamic loads of Load Case 2 governed the design loading for the walls perpendicular to the tsunami flow (Eq. (5)) and the flow stagnation loads (of the outgoing flow) governed the design of the parallel walls (Eq. (6)). Failure of the larger and smaller wall panels was calculated. The design loading was compared to the calculated capacity of the 120 mm thick wall panels and design

pressures were found to be conservatively high compared to the observed behavior in the building. The conservatism is associated with a high velocity estimate of around 1.5 times the estimated velocity from video analysis.

The walls were investigated with an assumed variation in the inundation depth and associated velocity at different assumed locations along the transect of the energy grade line. The calculated demand to capacity ratios for the walls at the different maximum inundation depths are provided in Fig. 5. For the larger panels the calculated inundation depth of 16.1m was 2.7 times the panel height and therefore Fig. 5b shows that failure was expected and design using the provisions of ASCE 7 would require a wall around 5 times stronger than its current capacity, with a thicker wall and much heavier reinforcing. The smaller walls that were not observed to fail would still be required to be around 2.5 times stronger for design. Therefore the design methodology is quite conservative compared to observed behavior. It would be an unusual building to be designed for a tsunami depth so much higher than the structure, as it would not function nor could it be used for life safety. For inundation depths that are more reasonable for the design of a building at around the height of the building, the observed concrete walls would be able to resist the hydrodynamic tsunami forces. The analysis does not consider debris impact forces, which may also need to be considered depending on the location and type of building.

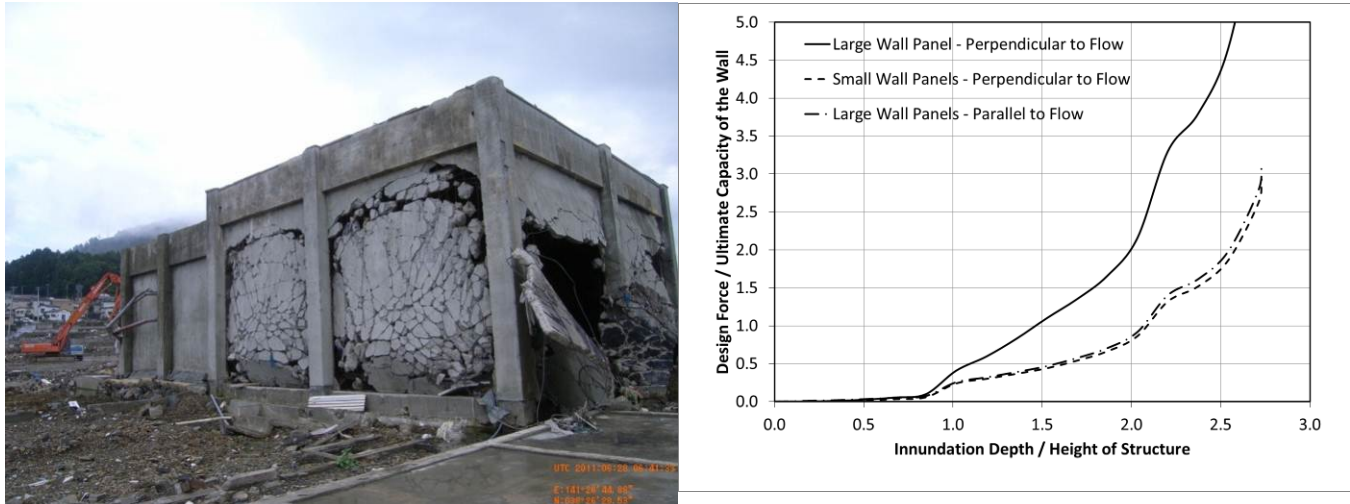


Fig. 5 - Onagawa concrete warehouse observed failure after the tsunami and design demand / wall capacity for different inundation depths and wall types in the building

### 3.6 Bore Conditions

The Minami Gamou Wastewater Treatment plant has a number of buildings and structures located on the Sendai coastline, south of the main port and approximately 330 m from the coastline. Video of this facility in Sendai showed a tsunami bore directly striking the longitudinal walls of buildings at the plant. Fig. 6 shows the ocean-facing wall of one particular building with a two-story high-bay on one side of the building that failed through out-of-plane flexure due to large hydrodynamic bore impact forces. The other side of the building did not fail, where the exposed exterior wall was laterally braced by a floor near the mid-height. The design of the walls in this building are considered with the application of ASCE 7 loading conditions.

While this condition with a bore striking a building during a tsunami is expected to be relatively rare, a larger Froude number coefficient is appropriate for the ASCE 7 standard. When the EGL analysis is performed with a Froude number coefficient of 1.3, based on the same inundation limit as observed during the tsunami, the resulting inundation depth at the site is calculated as 8.2 m and velocity is 11.1m/s [5]. Considering two-thirds of the maximum inundation depth, when using ASCE 7 Load Case 2, results in a height of 5.5 m, which is marginally less than the observed bore height of 6.0 m. The calculated velocity is 70% larger than the velocity estimated from video analysis at 6.7 m/s [16], therefore the overall calculated design force is conservatively



higher than the actual force experienced by the wall. The previous analysis showed that the wall failed at a force of around 780 kN/m, while the calculated design load per ASCE 7 for this condition is 1150 kN per meter length of the wall.

Options for strengthening the wall of the building were considered. If it was a new design reorienting the building 45 degrees so that the face of the building was not directly facing the shoreline would help to reduce forces on the exposed walls. However, as the bore is considered to strike from a direction at an angle that varies by 22.5 degrees either way from a transect perpendicular to the shoreline, the reorientation would only reduce design forces by around 8%. Another option may be to put horizontal struts in the high bay, although it would change the functionality of the space. As the vertical strength of the wall is provided by the pilasters spaced every 5.0m, strengthening these is the most effective way of strengthening the wall while maintaining the high bay. Calculations show that the existing 900 x 700 mm pilasters would need to be increase to around 1300 x 800 to resist the calculated tsunami load, with an increase in reinforcing from 0.6% to 2% at the base of the pilaster and associated portion of wall and increase in reinforcing yield strength from 300 MPa to 420 MPa. While this is a large local increase in the pilaster sizes, the area that requires the strengthening is a relatively small section of the building. During drawdown, bore conditions need not be considered, so a similar wall facing inland would not need the same level of strengthening.



Fig. 6 - Ocean-facing reinforced concrete wall at the Minami Gamou Wastewater Treatment Plant pump station building damaged by direct strike from tsunami bore (a) exterior view, (b) interior view

#### 4. Conclusions

Damaged buildings in the Tohoku region of Japan provided numerous examples of the structural response to various types of tsunami loading. The modifications of select buildings using the ASCE 7 tsunami design methodology to upgrade them to withstand equivalent tsunami inundation depths have been studied. Overall, the analyses from the Tohoku Tsunami demonstrate that ASCE 7 has developed sufficiently reliable tools for structural load characterization arising from suitably defined tsunami flow conditions. In general where the building is significantly overtopped it is difficult, and not logical, to economically design a reinforced concrete or steel building to survive the tsunami. However, where the inundation height is less than or up to the height of the building it is very feasible and practical to design reinforced concrete and structural steel frames to withstand tsunami design forces, particularly buildings that have an inherent systemic capacity accruing from seismic design requirements.

#### 5. Acknowledgments

The support of the American Society of Civil Engineers and the National Science Foundation (through NSF Rapid Grants 1138710 and 1138699) for the post-tsunami reconnaissance teams is greatly appreciated. We would also like to acknowledge the assistance of Kwok-Fai Cheung and Yoshiki Yamazaki in providing



topographical data for the energy grade line transects and Michael Olsen, Evon Silvia and Shawn Butcher for LIDAR data collection and synthesis.

## 6. References

- [1] The 2011 Tohoku Tsunami Joint Survey Group (2011): Nationwide Field Survey of the 2011 Off the Pacific Coast of Tohoku Earthquake Tsunami, *Journal of Japan Society of Civil Engineers, Series B*, **67** (1), 63-66.
- [2] National Institute for Land and Infrastructure Management / Building Research Institute (2011): Summary of the Field Survey and Research on “The 2011 of the Pacific coast of Tokoku Earthquake” (the Great East Japan Earthquake), *Technical Note of NILIM No. 647/ BRI Research Paper No. 150*.
- [3] Chock, G., Robertson, I., Kriebel, D., Francis, M., Nistor, I. (2013a): *Tohoku Japan Tsunami of March 11, 2011 – Performance of Structures under Tsunami Loads*. American Society of Civil Engineers, Structural Engineering Institute.
- [4] Maruyama, Y., Kitamura, K., Yamazaki, F. (2013): Estimation of Tsunami-Induced Areas in Asahi City, Chiba Prefecture, after than 2011 Tohoku-Oki Earthquake. *Earthquake Spectra*, **29** (S1), S201-S217.
- [5] Carden, L., Chock, G., Yu, G., and Robertson, I. (2015): The New ASCE Tsunami Design Standard Applied to Mitigate Tohoku Tsunami Building Structural Failure Mechanisms, *Chapter 22, Handbook of Coastal Disaster Mitigation for Engineers and Planners*, ed. By Esteban, M., Takagi, H., and Shibayama, T., Elsevier ISBN: 978-0-12-801060-0.
- [6] Akiyama, M., Frangopol, D.M., Arai, M., Koshimura, S. (2013) Reliability of Bridges under Tsunami Hazards: Emphasis on the 2011 Tohoku-Oki Earthquake, *Earthquake Spectra*, **29**(S1), p. S295-S314.
- [7] Kawashima, K., Buckle, I. (2013): Structural Performance of Bridges under Tsunami Hazards: Emphasis on the 2011 Tohoku-Oki Earthquake. *Earthquake Spectra*, **29** (S1), S315-S338.
- [8] Koshimura, S., Hayashi, S. (2012): Interpretation of Tsunami Flow Characteristics by Video Analysis. *9th International Conference on Urban Earthquake Engineering/ 4th Asia Conference on Earthquake Engineering*, Tokyo Institute of Technology, Tokyo.
- [9] Foytong, P., Ruangrassamee, A., Shoji, G., Hiraki, Y., Ezura, Y. (2013): Analysis of Tsunami Flow Velocities during the March 2011 Tohoku, Japan Tsunami. *Earthquake Spectra*, **29** (S1), S161-S181.
- [10] Liu, W., Yamazaki, F., Gokon, H., Koshimura, S. (2013): Extraction of Tsunami-Flooded Areas and Damaged Buildings in the 2011 Tohoku-Oki Earthquake from TerraSAR-X Intensity Images. *Earthquake Spectra*, **29**(S1), p. S183-S200.
- [11] Olsen, M.J., Carden, L.P., Silvia, E.P., Chock, G., Robertson, I.N., and Yim, S. (2012a): Capturing the Impacts: 3D Scanning after the 2011 Tohoku Earthquake and Tsunami. *9th International Conference on Urban Earthquake Engineering/ 4th Asia Conference on Earthquake Engineering*, Tokyo Institute of Technology, Tokyo, Japan.
- [12] Robertson, I.N., Chock, G., and Morla, J.P. (2012): Structural analysis of selected failures caused by the February 27, 2010 Chile Tsunami, *Earthquake Spectra*, **28** (S1), S215-S243.
- [13] Olsen, M.J., Cheung, K.F., Yamazaki, Y., Butcher, S.M., Garlock, M., Yim, S.C., McGarity, S., Robertson, I., Burgos L., and Young Y.L., (2012b): Damage Assessment of the 2010 Chile Earthquake and Tsunami using Terrestrial Laser Scanning, *Earthquake Spectra*, **28** (S1), S179-S197.
- [14] Geist, E. (2005): Local Tsunami Hazards in the Pacific Northwest from Cascadia Subduction Zone Earthquakes, *U.S. Geological Survey Professional Paper #1661-B*.
- [15] American Society of Civil Engineers/Structural Engineering Institute (2016) ASCE/SEI 7–16 Minimum Design Loads for Buildings and Other Structures. ASCE, Reston, Virginia.
- [16] Chock, G., Carden, L., Robertson, I., Olsen, M., Yu, G. (2013b): Tokoku Tsunami-Induced Building Failure Analysis with Implications for U.S. Tsunami and Seismic Design Codes. *Earthquake Spectra*, **29** (S1), S99-S126.